Inorg. Chem. **2007**, *46*, 2249–2260

Theoretical Investigations on Heteronuclear Chalcogen–Chalcogen Interactions: On the Nature of Weak Bonds between Chalcogen Centers

Christian Bleiholder,[†,‡] Rolf Gleiter,*[,†] Daniel B. Werz,[†,¶] and Horst Köppel[#]

Organisch-Chemisches Institut der Universität Heidelberg, Im Neuenheimer Feld 270, D-69120 Heidelberg, Germany, Deutsches Krebsforschungszentrum (DKFZ), Im Neuenheimer Feld 280, D-69120 Heidelberg, Germany, Institut für Organische und Biomolekulare Chemie der Universität Göttingen, Tammannstr. 2, D-37077 Göttingen, Germany, and Physikalisch-Chemisches Institut der Universität Heidelberg, Im Neuenheimer Feld 229, D-69120 Heidelberg, Germany

Received November 6, 2006

To understand the intermolecular interactions between chalcogen centers (O, S, Se, Te), quantum chemical calculations on model systems were carried out. These model systems were pairs of monomers of the composition $(CH_3)_2X_1$ (X_1 = O, S, Se, Te) as the donors and CH_3X_2Z (with X_2 = O, S, Se, Te and Z = Me, CN) as the acceptors. The variation of X_1, X_2, and Z leads to 32 pairs with 8 homonuclear cases ($X_1 = X_2$ = O, S, Se, Te) and 24 heteronuclear cases ($X_1 \neq X_2$). The MP2/SDB-cc-pVTZ, 6-311G* level of theory was used to derive the geometrical parameters and the interaction energies of the model systems. The pairs with Z = CN (**17**–**32**) show a considerably higher interaction energy than the pairs with CH_3 groups only (**1**–**16**). Natural bond orbital (NBO) analysis revealed that the interaction of the dimers **1**, **2**, **5**, **6**, **9**, **10**, **13**, **14**, **17**, **21**, **25**, and **29** is mainly due to weak hydrogen bonding between methyl groups and chalcogen centers. These systems all contain hard chalcogen atoms as acceptors. For all other systems, the chalcogen–chalcogen interaction dominates. The one-electron picture of an interaction between the lone pair of the donor chalcogen atom and the chalcogen–carbon antibonding σ^* orbital serves as a model to qualitatively rationalize trends found in many of these systems. However, it has to be applied with some amount of skepticism. A detailed analysis based on symmetry-adapted perturbation theory (SAPT) reveals that induction and dispersion forces dominate and contribute to the bonding in each case. Hydrogen-bonded compounds involve bonding electrostatic contributions. Compounds dominated by chalcogen–chalcogen interactions exhibit bonding due to electrostatic interactions only if one of the chalcogen atoms involved is sulfur or oxygen.

Introduction

Noncovalent bonding interactions play a major role in determining the structure of larger molecules. In macromolecular compounds such as proteins[1−3] and polysaccharides,[4,5] these rather weak forces are ubiquitous and, consequently, govern, to a vast extent, their secondary and tertiary structures. The most important noncovalent forces are ascribed to conventional hydrogen bonding (e.g., NH···O, OH···O).[1−5] Intensive structural investigations in the fields of biopolymers and organic conductors have unraveled that less common interactions such as nonconventional hydrogen bonds (CH···O, CH···π)[6,7] or interactions between chalcogen centers[8] contribute considerably to stabilize conformations.

The intermolecular interactions in compounds with covalently bound sulfur provide evidence for the directionality of this interaction.[8] Earlier results were interpreted in terms of donor−acceptor interactions.[9] Later on, the directional

* To whom correspondence should be addressed. E-mail: rolf.gleiter@oci.uni-heidelberg.de.
† Organisch-Chemisches Institut der Universität Heidelberg.
‡ DKFZ.
¶ Institut für Organische und Biomolekulare Chemie der Universität Göttingen.
# Physikalisch-Chemisches Institut der Universität Heidelberg.

(1) Pauling, L.; Corey, R. B. *Proc. Natl. Acad. Sci. U.S.A.* **1951**, *37*, 251−256.
(2) Pauling, L.; Corey, R. B. *Proc. Natl. Acad. Sci. U.S.A.* **1951**, *37*, 729−740.
(3) Pauling, L.; Corey, R. B.; Branson, H. R. *Proc. Natl. Acad. Sci. U.S.A.* **1951**, *37*, 205−211.
(4) (a) Casu, B.; Reggiani, M.; Gallo, G. G.; Vigevani, A. *Tetrahedron* **1966**, *22*, 3061−3083. (b) Ellis, J. W.; Bath, J. *J. Am. Chem. Soc.* **1940**, *62*, 2859−2861.
(5) Banks, W.; Greenwood, C. T. *Biopolymers* **1972**, *11*, 315−318.

10.1021/ic062110y CCC: $37.00
Published on Web 02/21/2007

bonding between two divalent chalcogen centers was traced back to an interaction between the occupied np lone pair at the donating chalcogen center and a chalcogen−carbon σ^* orbital of the accepting center.[10]

Interactions between closed-shell molecules of period 3 and higher have been modeled by quantum chemical methods.[11] Semiempirical methods were applied in the earlier days;[12] later on, HF−SCF[13] and DFT[14] procedures were used. To understand the nature of chalcogen−chalcogen interactions in organic donor molecules such as tetrathiafulvalene (TTF), model studies were carried out on the dimers $H_2X\cdots XH_2$ with X = O, S, Se, Te at the MP2 level of theory using the 6-311G(d,p), 6-311G(2d,2p), and 6-311G(3df,3pd) basis sets.[15] Only one angle and the X···X distance were varied, yielding only a weak angular dependence. This suggested that a D_{2h} arrangement is reasonable in describing the X···X interactions.[15]

The intermolecular distances in the dimeric hydrides $(HE-EH)_2$ (E = Se, Te, Po) could be reproduced at the MP2 level of theory.[16] Inspired by recent studies on dimethyldichalcogenanes[17] and by our observations that cyclic systems with divalent chalcogen atoms form columnar structures and even nanotubes via intermolecular chalcogen−chalcogen interactions,[18] we were interested in the nature of noncovalent interactions between chalcogen centers. Quantum chemical calculations on molecules with homoatomic pairs of chalcogen atoms such as **1**, **6**, **11**, **16**, **17**, **22**, **27**, and **32** (Chart 1) were used for our model studies.[19] It was found that, for the lighter chalcogen centers, especially with two methyl groups at the accepting unit (e.g., **1**, **6**, **11**), weak hydrogen bonding between the methyl groups and the chalcogen centers dominates.[19] For the homoatomic aggregates with heavier chalcogen centers (**16**) and for those with an electron-withdrawing acceptor substituent (**22**, **27**, **32**), the chalco-

Chart 1. Dimeric Model Systems **1**−**32**

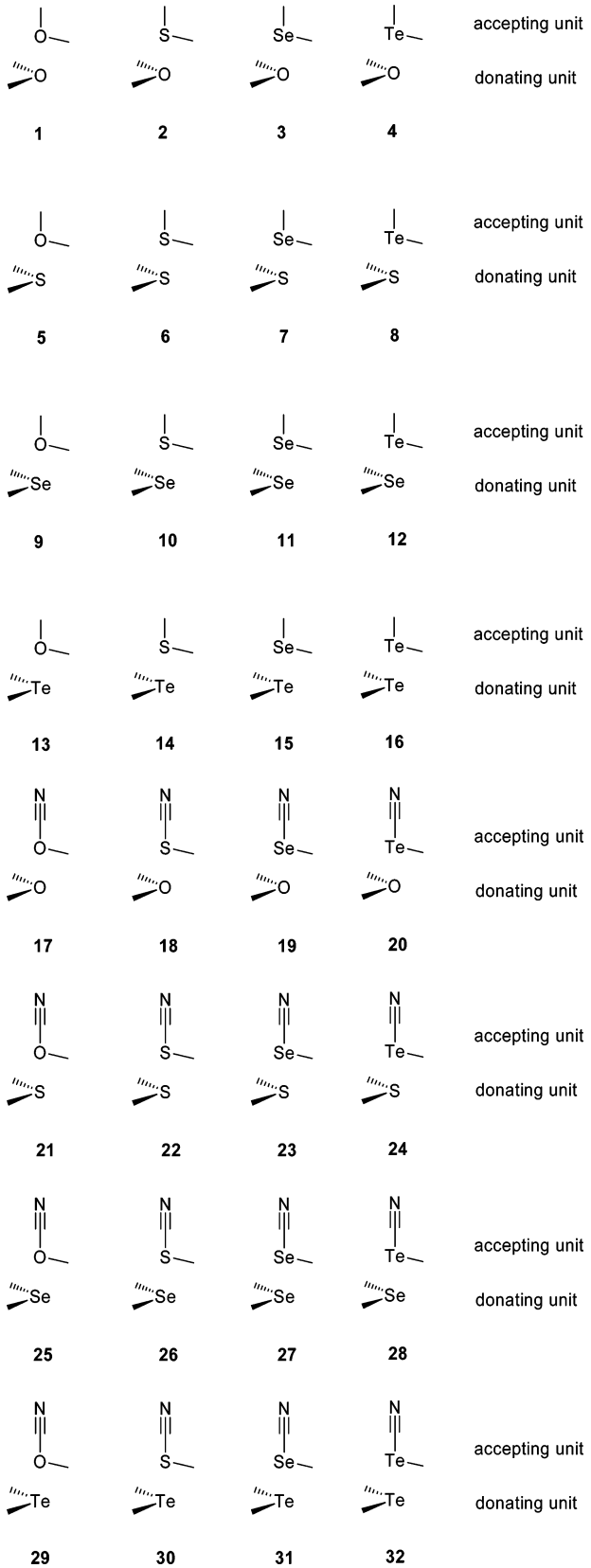

(6) (a) Desiraju, G. R.; Steiner, T. *The Weak Hydrogen Bond*; Oxford University Press: New York, 1999. (b) Steiner, T. *Angew. Chem.* **2002**, *114*, 51−80. (c) Steiner, T. *Angew. Chem., Int. Ed.* **2002**, *41*, 48−78.
(7) Nishio, M.; Hirota, M.; Umezawa, Y. *The CH/π-Interaction*; Wiley-VCH: New York, 1998.
(8) (a) Williams, J. M.; Ferraro, J. R.; Thorn, R. J.; Carlson, K. D.; Geier, U.; Wang, H. H.; Kini, A. M.; Whangbo, M.-H. *Organic Superconductors*; Prentice Hall: Englewood Cliffs, NJ, 1992. (b) Iwaoka, M.; Takemoto, S.; Okada, M.; Tomoda, S. *Bull. Chem. Soc. Jpn.* **2002**, *75*, 1611−1625.
(9) Bent, H. A. *Chem. Rev.* **1968**, *68*, 587−648.
(10) (a) Rosenfield, R. E.; Parthasarathy, R.; Dunitz, J. D. *J. Am. Chem. Soc.* **1977**, *99*, 4860−4862. (b) Glusker, J. P. *Top. Curr. Chem.* **1998**, *198*, 1−56. (c) Guru Row, T. N.; Parthasarathy, R. *J. Am. Chem. Soc.* **1981**, *103*, 477−479. (d) Ramasubbu, N.; Parthasarathy, R. *Phosphorus, Sulfur Silicon Relat. Elem.* **1987**, *31*, 221−229.
(11) Pyykkö, P. *Chem. Rev.* **1997**, *97*, 597−636 and references cited therein.
(12) Boyd, D. B. *J. Phys. Chem.* **1978**, *82*, 1407−1416.
(13) Ángyán, J. G.; Poirier, R. A.; Kucsman, A.; Csizmadia, I. G. *J. Am. Chem. Soc.* **1987**, *109*, 2237−2245.
(14) Sanz, P.; Yáñez, M.; Mó, O. *J. Phys. Chem. A* **2002**, *106*, 4661−4668.
(15) Novoa, J. J.; Whangbo, M.-H.; Williams, J. M. In *Organic Superconductivity*; Kresin, V. Z., Little, W. A., Eds.; Plenum Press: New York, 1990; pp 231−242.
(16) Klinkhammer, K. W.; Pyykkö, P. *Inorg. Chem.* **1995**, *34*, 4134−4138.
(17) Mundt, O.; Becker, G.; Baumgarten, J.; Riffel, H.; Simon, A. *Z. Anorg. Allg. Chem.* **2006**, *632*, 1687−1709.
(18) (a) Werz, D. B.; Staeb, T. H.; Benisch, C.; Rausch, B. J.; Rominger, F.; Gleiter, R. *Org. Lett.* **2002**, *4*, 339−342. (b) Werz, D. B.; Gleiter, R.; Rominger, F. *J. Am. Chem. Soc.* **2002**, *124*, 10638−10639. (c) Werz, D. B.; Rausch, B. J.; Gleiter, R. *Tetrahedron Lett.* **2002**, *43*, 5767−5769. (d) Gleiter, R.; Werz, D. B.; Rausch, B. J. *Chem.−Eur. J.* **2003**, *9*, 2676−2683. (e) Werz, D. B.; Gleiter, R.; Rominger, F. *Organometallics* **2003**, *22*, 843−849. (f) Schulte, J. H.; Werz, D. B.; Gleiter, R. *Org. Biomol. Chem.* **2003**, *1*, 2788−2794. (g) Werz, D. B.; Gleiter, R.; Rominger, F. *J. Org. Chem.* **2004**, 69, 2945−2952. (h) Gleiter, R.; Werz, D. B. *Chem. Lett.* **2005**, *34*, 126−131.
(19) Bleiholder, C.; Werz, D. B.; Köppel, H.; Gleiter, R. *J. Am. Chem. Soc.* **2006**, *128*, 2666−2674.

gen−chalcogen interactions prevail. A detailed analysis based on symmetry-adapted perturbation theory (SAPT) revealed[19] that the nature of the noncovalent interaction in these model systems depends crucially on the type of chalcogen element involved. For the homoatomic oxygen-containing compounds (such as **1** and **17**), both electrostatic- and dispersion-type forces contribute significantly to the bonding. This is in contrast to the findings for the compounds containing the heavier element Te. Here, the interaction is dominated by dispersion, while electrostatic forces actually act in an antibonding manner. Also, a dependence on the very type of the substituent Z in the accepting unit was observed. An electron-withdrawing group (EWG) increased the electrostatic bonding in the oxygen-containing compounds while keeping dispersion constant. Also, this is found to be in contradiction with the trends observed for the heavier chalcogens, for which an EWG increased both the bonding and the antibonding contributions due to dispersion- and electrostatic-type forces, respectively. A transition in the nature of the noncovalent bonding between these extrema was observed when going from O to Te via S and Se. On the basis of these findings, it was concluded that, in contacts between oxygen-containing compounds, (nonconventional) hydrogen bonding prevails. However, when the heavier element Te is involved, the bonding is dominated by interactions between the chalcogen atoms. For S and Se, a transition between these extrema was observed, depending on the actual substituents located on the chalcogen atoms.

It is, thus, of high interest to investigate the nature of noncovalent interactions taking place between two different chalcogen elements. In this work, we extend our previous study with model systems of heteroatomic interactions (**2**−**5**, **7**−**10**, **12**−**15**, **18**−**21**, **23**−**26**, and **28**−**31**) (as depicted in Chart 1). It is noteworthy that always 2 of the first 16 model systems can be viewed as different conformers (i.e., **2** and **5**).

The present investigations were also stimulated by various discussions on interactions between different chalcogen atoms in the literature. Noncovalent interactions between two different chalcogen atoms have long attracted scientific interest.[20] Most prominent examples of heteroatomic chalcogen−chalcogen interactions investigated are S···X (X = O, S, Se),[8b,21a,b,d] O···X (X = S, Se, Te),[21c] O···Se,[22a] and S···Te[22b] interactions. Related to these studies were reports on chalcogen−nitrogen interactions in diatomic chalcogenides,[23] Se···N[24] and Te···N[25] species. In this field, there also belongs a report that O···Se interactions in selenazole nucleosides may play a major role in the antitumor and antiviral activity of these compounds.[26]

As in our previous studies,[19] we base our considerations on three different approaches. To obtain accurate interaction energies and the geometrical parameters of the energetic minimum, we used the supermolecular approach. Perturbation theoretical calculations were performed to investigate the electronic origin of the interaction. The principal interacting groups, such as chalcogen−chalcogen contacts and weak hydrogen bonding, were identified by means of NBO analysis.

Computational Details

Definition of Interaction Energy. Throughout this paper, we use the term "interaction energy" as previously defined (eq 1)[19]

$$E_{\mathrm{int}}(\vec{r},\vec{\xi},\vec{Q}_A,\vec{Q}_B) = E_{AB}(\vec{r},\vec{\xi},\vec{Q}_A,\vec{Q}_B) - E_A(\vec{Q}_A) - E_B(\vec{Q}_B) \quad (1)$$

This equation defines the interaction energy (E_{int}) as the difference between the energy of a supermolecule E_{AB} and the separated monomers (E_A, E_B), where the monomers have the same internal coordinates (Q_A, Q_B) as the supermolecule. The relative orientation of the monomers is described using the intermolecular vector $\vec{r}$ and the orientational angles $\vec{\xi}$. Unless otherwise noted, all quantities in this work are corrected for basis set superposition error (BSSE) using the counterpoise (CP) procedure.[27] The interaction energies are denoted as $E_{\mathrm{int,method}}^{\mathrm{basis}}$. It should be noted that the interaction energy defined according to eq 1 cannot take into account zero-point corrections.

Choice of Basis Sets and Methods. Selection of the basis set proved to be difficult for our purposes. Several studies have revealed that at least a polarization or diffuse augmented split-valence triple-ζ basis set in combination with electron-correlation methods is needed to obtain reliable results for van der Waals-type interactions.[28] Additionally, a good effective core potential (ECP) was needed, at least for tellurium-containing compounds. Hence, we chose the family of Dunning's correlation-consistent basis sets (correlation-consistent polarized valence triple-ζ, cc-pVTZ, cc-pVTZ-PP, SDB-cc-pVTZ[29,30]) for which high-quality, small- and large-core ECPs have recently been derived. Benchmarking was done in an earlier study[19] using these basis sets combined with Pople's 6-311G family for the lighter atoms (H, C, N)[31] with and without polarization and diffuse functions, in combination with a variety

(20) (a) Gleiter, R.; Gygax, R. *Top. Curr. Chem.* **1976**, *63*, 49−88. (b) Vargas-Baca, I.; Chivers, T. *Phosphorus, Sulfur Silicon Relat. Elem.* **2000**, *164*, 207−227.

(21) (a) Iwaoka, M.; Takemoto, S.; Okada, M.; Tomoda, S. *Chem. Lett.* **2001**, *2*, 132−133. (b) Pal, D.; Chakrabarti, P. *J. Biomol. Struct. Dyn.* **2001**, *19*, 115−128. (c) Minyaev, R. M.; Minkin, V. I. *Can. J. Chem.* **1998**, *76*, 776−788. (d) Tiecco, M.; Testaferri, L.; Santi, C.; Tomassini, C.; Santoro, S.; Marini, F.; Bagnoli, L.; Temperini, A.; Costantino, F. *Eur. J. Org. Chem.* **2006**, 4867−4873.

(22) (a) Barton, D. H. R.; Hall, M. B.; Lin, Z.; Parekh, S. I.; Reibenspies, J. *J. Am. Chem. Soc.* **1993**, *115*, 5056−5059. (b) Fleischer, H.; Mitzel, N. W.; Schollmeyer, D. *Eur. J. Inorg. Chem.* **2003**, *5*, 815−821.

(23) (a) Kontopoulos, C.; Sigalas, M. P. *J. Mol. Struct.: THEOCHEM* **1999**, *490*, 125−131. (b) Allan, R. E.; Gornitzka, H.; Kärcher, J.; Paver, M. A.; Rennie, M.-A.; Russell, C. A.; Raithby, O. R.; Stalke, D.; Steiner, A.; Wright, D. S. *J. Chem. Soc., Dalton. Trans.* **1996**, 1727−1730.

(24) (a) Fujihara, H.; Tanaka, H.; Furukawa, N. *J. Chem. Soc., Perkin Trans. 1* **1995**, 2375−2377. (b) Iwaoka, M.; Tomoda, S. *Phosphorous, Sulfur Silicon Relat. Elem.* **1992**, *67*, 125−130.

(25) Cozzolino, A. F.; Vargas-Baca, I.; Mansour, S.; Mahmoudkhani, A. H. *J. Am. Chem. Soc.* **2005**, *127*, 3184−3190.

(26) Burling, F. T.; Goldstein, B. M. *J. Am. Chem. Soc.* **1992**, *114*, 2313−2320.

(27) Boys, S. F.; Bernardi, F. *Mol. Phys.* **1970**, *19*, 553−566.

(28) DelBene, J. E.; Shavitt, I. In *Molecular Interactions*; Scheiner, S., Ed.; John Wiley & Sons: New York, 1997; pp 157−179.

(29) (a) Dunning, T. H., Jr.; Thom, H.; Peterson, K. A. In *Encyclopedia of Computational Chemistry*; Schleyer, P. v. R., Ed.; Wiley: New York, 1998; Vol. 1, pp 88−115. (b) Dunning, T. H., Jr. *J. Chem. Phys.* **1989**, *90*, 1007−1023. (c) Peterson, K. A. *J. Chem. Phys.* **2003**, *119*, 11099−11112. (d) Peterson, K. A.; Figgen, D.; Goll, E.; Stoll, H.; Dolg, M. *J. Chem. Phys.* **2003**, *119*, 11113−11123. (e) Metz, B.; Schweizer, M.; Stoll, H.; Dolg, M.; Liu, W. *Theor. Chem. Acc.* **2000**, *104*, 22−28. (f) Metz, B.; Stoll, H.; Dolg, M. *J. Chem. Phys.* **2000**, *113*, 2563−2569. (g) Martin, J. M. L.; Sundermann, A. *J. Chem. Phys.* **2001**, *114*, 3408−3420. (h) Bergner, A.; Dolg, M.; Kuechle, W.; Stoll, H.; Preuss, H. *Mol. Phys.* **1993**, *80*, 1431−1441.

of electronic structure methods (HF,[32] MPn,[33] CCSD(T),[34] B3LYP[35]). In this study, we varied the distance between the two chalcogen centers of four small model compounds, leaving all other geometrical parameters fixed.[19] This investigation revealed that the MP2/SDB-cc-pVTZ, 6-311G* as well as the MP3/SDB-aug-cc-pVTZ, 6-311++G** levels of theory provide a very efficient way for estimating the coupled cluster CCSD(T)/aug-cc-pVTZ-PP, 6-311++G** interaction energies. The SDB-cc-pVTZ, 6-311G* basis set is denoted as cc-pVTZ-ECP, and SDB-aug-cc-pVTZ, 6-311++G** is denoted as aug-cc-pVTZ-ECP. The Hartree−Fock (HF) level of theory turned out to be insufficient for describing the interaction between two divalent chalcogens and led to supermolecule geometries with intermolecular distances that were too long. However, it predicted a bonding interaction between the two chalcogen centers. (See ref 19 for details.)

For the model systems shown in Chart 1, we optimized the geometrical parameters with Gaussian03[36] using the counterpoise protocol to obtain BSSE-corrected[37] supramolecular geometries. Each geometry has been characterized as a minimum by a subsequent frequency calculation.

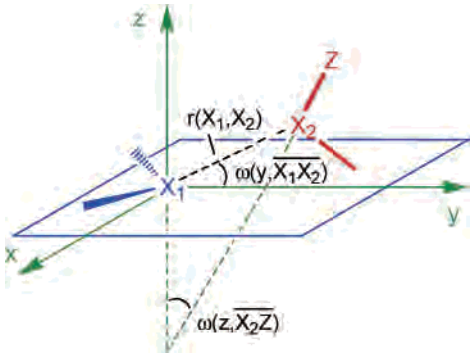

Figure 1. Definition of the three most important parameters: the distance $r(X_1,X_2)$ and the orientational angles $\omega(y,\overline{X_1X_2})$ and $\omega(z,\overline{X_2Z})$, which have been used to characterize the optimized geometries of **1**−**32** in Table 1.

Special attention was paid to the flatness of a van der Waals potential energy surface (PES). Therefore, the convergence criteria during geometry optimizations were set rather tight to reach the minima as closely as possible (maximum gradient 15×10^{-6} au/α_0; rms gradient 10×10^{-6} au/α_0; maximum displacement 60×10^{-6} α_0; rms displacement 40×10^{-6} α_0). Additionally, force constants were recalculated every 5−10 steps. Perturbation theoretical interaction energy corrections were computed using SAPT2002.[38] For these calculations, Atmol1024[39] was used as the necessary SCF front end. In order to include the tellurium-containing model systems in the SAPT calculations, the DGDZVP[40] basis set was chosen here. The SAPT/DGDZVP calculations were performed on the dimer's optimized geometries at the MP2/DGDZVP level of theory. However, careful benchmarking between the MP2/cc-pVTZ-ECP, CCSD(T)/DGDZVP, SAPT/DGDZVP, and SAPT/6-311G** revealed that, by using the rather small DGDZVP basis set, no qualitative error was introduced into the SAPT calculations (see Supporting Information for details). The energy corrections calculated by the SAPT program have been summed up to give the electrostatic, induction, dispersion, as well as the exchange correlation contributions according to eqs 4−7[19] (see the SAPT paragraph).

NBO analyses[41] were employed to estimate the relative amount of hydrogen bonding compared to chalcogen−chalcogen interactions. To this end, NBO analyses were performed on the dimer's optimized geometries using the HF/aug-cc-pVTZ-ECP density. Each intermonomer NBO interaction term was interpreted in terms of

(30) Basis sets were partly obtained from the Extensible Computational Chemistry Environment Basis Set Database, Version 02/25/04, as developed and distributed by the Molecular Science Computing Facility, Environmental and Molecular Sciences Laboratory which is part of the Pacific Northwest Laboratory, P.O. Box 999, Richland, Washington 99352, U.S.A. and is funded by the U.S. Department of Energy. The Pacific Northwest Laboratory is a multiprogram laboratory operated by Battelle Memorial Institute for the U.S. Department of Energy under Contract DE-AC06−76.RLO 1830. Contact Karen Schuchardt for further information.

(31) (a) Krishnan, R.; Binkley, J. S.; Seeger, R.; Pople, J. A. *J. Chem. Phys.* **1980**, *72*, 650−654. (b) McLean, A. D.; Chandler, G. S. *J. Chem. Phys.* **1980**, *72*, 5639−5648. (c) Curtiss, L. A.; McGrath, M. P.; Blaudeau, J.-P.; Davis, N. E.; Binning, R. C., Jr.; Radom, L. *J. Chem. Phys.* **1995**, *103*, 6104−6113. (d) Clark, T.; Chandrasekhar, J.; Spitznagel, G. W.; Schleyer, P. v. R. *J. Comput. Chem.* **1983**, *4*, 294−301.

(32) (a) Hartree, D. R. *The Calculation of Atomic Structure*; Wiley: New York, 1957. (b) Roothaan, C. J. J. *Rev. Mod. Phys.* **1960**, *32*, 179−185. (c) Huzinaga, S. *Phys. Rev.* **1960**, *120*, 866−871. (d) Huzinaga, S. *Phys. Rev.* **1961**, *122*, 131−138. (e) Veszprémi, T.; Fehér, M. *Quantum Chemistry: Fundamentals to Applications*: Plenum Publishing: New York, 1999.

(33) (a) Møller, C.; Plesset, M. S. *Phys. Rev.* **1934**, *46*, 618−622. (b) Pople, J. A.; Seeger, R.; Krishnan, R. *Int. J. Quantum. Chem.* **1977**, *11*, 149−163. (c) Pople, J. A.; Binkley, J. S.; Seeger, R. *Int. J. Quantum. Chem.* **1976**, *10*, 1−19.

(34) (a) Pople, J. A.; Krishnan, R.; Schlegel, H. B.; Binkley, J. S. *Int. J. Quantum. Chem.* **1978**, *14*, 545−560. (b) Bartlett, R. J.; Purvis, G. D. *Int. J. Quantum. Chem.* **1978**, *14*, 561−581. (c) Cizek, J. *Adv. Chem. Phys.* **1969**, *14*, 35−45. (d) Purvis, G. D.; Bartlett, R. J. *J. Chem. Phys.* **1982**, *76*, 1910−1918. (e) Scuseria, G. E.; Janssen, C. L.; Schaefer, H. F., III. *J. Chem. Phys.* **1988**, *89*, 7382−7387. (f) Scuseria, G. E.; Schaefer, H. F., III. *J. Chem. Phys.* **1989**, *90*, 3700−3703. (g) Pople, J. A.; Head-Gordon, M.; Raghavachari, K. *J. Chem. Phys.* **1987**, *87*, 5968−5975.

(35) (a) Lee, C.; Yang, W.; Parr, R. G. *Phys. Rev. B* **1988**, *37*, 785−789. (b) Miehlich, B.; Savin, A.; Stoll, H.; Preuss, H. *Chem. Phys. Lett.* **1989**, *157*, 200−206. (c) Becke, A. D. *J. Chem. Phys.* **1993**, *98*, 5648−5652.

(36) Frisch, M. J.; Trucks, G. W.; Schlegel, H. B.; Scuseria, G. E.; Robb, M. A.; Cheeseman, J. R.; Montgomery, J. A., Jr.; Vreven, T.; Kudin, K. N.; Burant, J. C.; Millam, J. M.; Iyengar, S. S.; Tomasi, J.; Barone, V.; Mennucci, B.; Cossi, M.; Scalmani, G.; Rega, N.; Petersson, G. A.; Nakatsuji, H.; Hada, M.; Ehara, M.; Toyota, K.; Fukuda, R.; Hasegawa, J.; Ishida, M.; Nakajima, T.; Honda, Y.; Kitao, O.; Nakai, H.; Klene, M.; Li, X.; Knox, J. E.; Hratchian, H. P.; Cross, J. B.; Bakken, V.; Adamo, C.; Jaramillo, J.; Gomperts, R.; Stratmann, R. E.; Yazyev, O.; Austin, A. J.; Cammi, R.; Pomelli, C.; Ochterski, J. W.; Ayala, P. Y.; Morokuma, K.; Voth, G. A.; Salvador, P.; Dannenberg, J. J.; Zakrzewski, V. G.; Dapprich, S.; Daniels, A. D.; Strain, M. C.; Farkas, O.; Malick, D. K.; Rabuck, A. D.; Raghavachari, K.; Foresman, J. B.; Ortiz, J. V.; Cui, Q.; Baboul, A. G.; Clifford, S.; Cioslowski, J.; Stefanov, B. B.; Liu, G.; Liashenko, A.; Piskorz, P.; Komaromi, I.; Martin, R. L.; Fox, D. J.; Keith, T.; Al-Laham, M. A.; Peng, C. Y.; Nanayakkara, A.; Challacombe, M.; Gill, P. M. W.; Johnson, B.; Chen, W.; Wong, M. W.; Gonzalez, C.; Pople, J. A. *Gaussian 03*, revision B.03; Gaussian, Inc.: Wallingford, CT, 2004.

(37) (a) van Duijneveldt, F. B.; van Duijneveldt-van de Rijdt, J. G. C. M.; van Lenthe, J. H. *Chem. Rev.* **1994**, *94*, 1873−1885. (b) Paizs, B.; Suhai, S. *J. Comput. Chem.* **1998**, *19*, 575−584. (c) Salvador, P.; Paizs, B.; Duran, M.; Suhai, S. *J. Comput. Chem.* **2001**, *22*, 765−786.

(38) Bukowski, R.; Cencek, W.; Jankowski, P.; Jeziorski, B. L.; Jeziorska, M. L.; Kucharski, S. A.; Misquitta, A. J.; Moszynski, R.; Patkowski, K.; Rybak, S.; Szalewicz, K.; Williams, H. L.; Wormer, P. E. S. *SAPT2002: An Ab Initio Program for Many-Body Symmetry-Adapted Perturbation Theory Calculations of Intermolecular Interaction Energies*; University of Delaware: Newark, DE and University of Warsaw: Warsaw, Poland, 2002.

(39) Saunders, V. R.; Guest, M. F. ATMOL Program Package (SERC) Daresbury Laboratory: Daresbury, Great Britain.

(40) (a) Sosa, C.; Andzelm, J.; Elkin, B. C; Wimmer, E.; Dobbs, K. D.; Dixon, D. A. *J. Phys. Chem.* **1992**, *96*, 6630−6636. (b) Godbout, N.; Salahub, D. R.; Andzelm, J.; Wimmer, E. *Can. J. Chem.* **1992**, *70*, 560−571.

(41) (a) Carpenter, J. E.; Weinhold, F. *J. Mol. Struct.: THEOCHEM* **1988**, *46*, 41−62. (b) Foster, J. P.; Weinhold, F. *J. Am. Chem. Soc.* **1980**, *102*, 7211−7218.

Table 1. Calculated Interaction Energies $E_{int,MP2}^{cc-pVTZ-ECP}$ [kcal/mol], Intermolecular Equilibrium Distance $r(X_1,X_2)$ [Å], Orientational Angles $\omega(y, \overline{X_1X_2})$ and $\omega(z,\overline{X_2Z})$ [deg], and the Change, $\Delta\tilde{\nu}_{symm}$ [cm^{-1}], in the Symmetric Stretching Mode of the X_2-C Bond of **1**−**32** Calculated at the MP2/cc-pVTZ-ECP Level of Theory

system	X_1	X_2	Z	$E_{int,MP2}^{cc-pVTZ-ECP}$ [b]	$r(X_1,X_2)$[a,b]	$\omega(y, \overline{X_1X_2})$[a,b]	$\omega(z,\overline{X_2Z})$[a,b]	$\Delta\tilde{\nu}_{symm}$[b]
1	O	O	Me	−2.15	3.68	113.8	29.0	4.6
2	O	S	Me	−2.41	3.46	84.5	10.3	−0.9
3	O	Se	Me	−2.53	3.37	76.1	23.3	0.7
4	O	Te	Me	−3.11	3.29	62.3	40.1	−0.2
5	S	O	Me	−2.89	3.96	130.1	52.0	−0.9
6	S	S	Me	−2.79	4.03	113.9	19.7	−1.5
7	S	Se	Me	−2.81	3.78	103.0	11.4	−0.3
8	S	Te	Me	−3.37	3.67	93.4	3.4	−1.1
9	Se	O	Me	−2.89	4.06	133.5	56.4	−1.3
10	Se	S	Me	−2.79	4.16	118.5	25.0	−2.5
11	Se	Se	Me	−2.82	3.91	108.1	19.0	−1.6
12	Se	Te	Me	−3.39	3.78	98.8	8.8	−1.8
13	Te	O	Me	−2.92	4.18	137.6	67.7	−0.7
14	Te	S	Me	−2.84	4.22	121.5	33.1	−2.6
15	Te	Se	Me	−2.88	4.08	114.6	26.0	−1.0
16	Te	Te	Me	−3.40	3.97	105.7	17.9	−3.4
17	O	O	CN	−2.95	3.43	94.2	12.8	−4.8
18	O	S	CN	−4.16	3.08	66.0	26.9	−5.4
19	O	Se	CN	−5.08	2.99	54.4	41.3	−12.1
20	O	Te	CN	−6.59	2.94	43.6	55.9	−16.6
21	S	O	CN	−2.95	3.80	118.2	43.4	−10.4
22	S	S	CN	−3.85	3.38	97.8	13.7	−6.6
23	S	Se	CN	−4.71	3.38	91.1	3.4	−15.9
24	S	Te	CN	−6.42	3.30	83.8	9.7	−24.7
25	Se	O	CN	−2.89	3.94	122.8	48.0	−10.5
26	Se	S	CN	−3.76	3.61	102.6	19.0	−7.6
27	Se	Se	CN	−4.62	3.50	96.9	10.7	−16.5
28	Se	Te	CN	−6.44	3.41	90.1	1.5	−26.8
29	Te	O	CN	−2.74	4.05	126.7	56.5	−10.3
30	Te	S	CN	−3.60	3.82	109.3	27.7	−7.6
31	Te	Se	CN	−4.38	3.71	103.8	20.2	−16.9
32	Te	Te	CN	−6.18	3.61	96.9	8.8	−29.0

[a] For the definition of the parameters, see Figure 1. [b] Corrected for BSSE.

hydrogen bonding or chalcogen−chalcogen interaction, depending on the atoms the NBO was placed upon. Finally, they were summed up to estimate the strength of the hydrogen bonding and chalcogen−chalcogen interaction. (See ref 19 for a detailed description of the summation algorithm.) Charge transfer between the two molecular units was also obtained from the NBO analysis. Because the charge q_i for each isolated unit is zero and $q_1 = -q_2$, the net charge transfer from molecular unit 2 to unit 1 is given by the charge of molecular unit 1.

Results and Discussion

Model Systems. Our model systems are the heterodimers listed in Chart 1, which we subdivided into two groups. In **1**−**16**, we consider only methyl groups on the donor and acceptor units. In **17**−**32**, one methyl group on the acceptor unit is replaced by a cyano group, with the intention of increasing the acceptor's electron-withdrawing properties. Our previous studies showed that one cyano group is sufficient to mirror acceptor properties. By including the homonuclear cases **1**, **6**, **11**, **16**, **17**, **22**, **27**, and **32**, each of the two groups can be subdivided into four families corresponding to the four chalcogen atoms in the dimer's accepting subunit with four pairs each.

Optimized Geometries and Supermolecular Interaction Energies. For the model systems **1**−**32**, we performed full geometry optimizations at the MP2/cc-pVTZ-ECP level of theory, as described previously in this Article. All internal parameters of the dimer, including Q_i, $r(X_1,X_2)$, and the orientational angles $\omega(y,\overline{X_1X_2})$ and $\omega(z,\overline{X_2Z})$, as defined in Figure 1, were optimized.

In Table 1, we list the calculated equilibrium distances $r(X_1,X_2)$, the interaction energies $E_{int,MP2}^{cc-pVTZ-ECP}$, the orientation angles $\omega(y,\overline{X_1X_2})$ and $\omega(z,\overline{X_2Z})$, and the change in the stretching vibration $\Delta\tilde{\nu}$ of the X_2-Z bond due to aggregation. The geometries of two representative model systems **3** and **32** are depicted in Figure 2. The aforementioned subdivision of the two groups into four families shows up when we look at the difference, Δr, between $r(X_1,X_2)$ and the sum of the van der Waals radii[42] for the chalcogen elements involved ($r_{vdW}(X_1)$ and $r_{vdW}(X_2)$): O···O 2.80, O···S 3.25, O···Se 3.40, O···Te 3.60, S···S 3.70, S···Se 3.85, Se···Se 4.00, S···Te 4.05, Se···Te 4.20, and Te···Te 4.40 Å).[42] This difference Δr is shown in Figure 3 for the donor−acceptor pairs **1**−**32**.

In each of the first four families (**1**−**16**), we always find two positive and two negative values for Δr (Figure 3). The cases having positive values for Δr are always those model systems having oxygen or sulfur in the accepting fragment, while for the cases having selenium or tellurium in the accepting subunit, the intermolecular distance $r(X_1,X_2)$ is always smaller than the sum of the particular van der Waals radii.

In the second group, in which one methyl substituent is replaced by the more electron-withdrawing cyano substituent,

(42) Pauling, L. *The Nature of the Chemical Bond*, 4th ed.; Cornell University Press: Ithaca, NY, 1973.

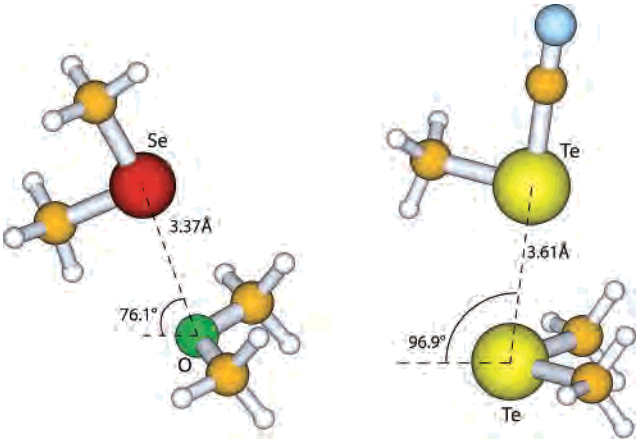

Figure 2. Geometries (ball and stick model) of the two model systems **3** (left) and **32** (right). Distances $r(X_1,X_2)$ and angles $\omega(y,\overline{X_1X_2})$ are indicated in the figure.

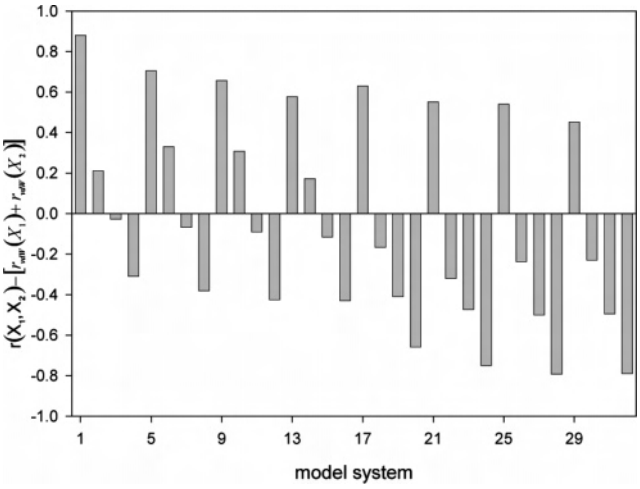

Figure 3. Difference between the calculated distances $r(X_1,X_2)$ and the sum of the van der Waals radii $r_{vdW(X_1)}$ and $r_{vdW(X_2)}$ of **1**−**32**.

only the first member of each family (**17**, **21**, **25**, and **29**) shows positive Δr values. However, all other values vary between −0.17 and −0.79 Å (Figure 3).

Taking a closer look at the trends within each group, it is found that Δr becomes smaller when the element X_2 in the accepting subunit is held constant (i.e., in the series **1**, **5**, **9**, **13** and **3**, **7**, **11**, **15**, etc.). Big exceptions are the two sulfur-containing series **2**, **6**, **10**, **14** and **18**, **22**, **26**, **30**. In the first series (**2**, **6**, **10**, **14**), we find a maximum of Δr for homoatomic system **6**, while in the second series (**18**, **22**, **26**, **30**), the homoatomic system **22** shows the smallest value. The specialty of the element sulfur with respect to the intermolecular interactions studied here is also indicated by the observation that the sign of Δr is determined by the substituent Z of the accepting subunit whenever its chalcogen atom is sulfur. For all other compounds, the sign of Δr is independent of Z, and Δr is either greater than zero (for the compounds having oxygen-containing acceptors) or smaller than zero (for the compounds having selenium- or tellurium-containing acceptors). These observations further support our previously made conclusion that the nature of the noncovalent interaction of the oxygen-containing compounds is principally distinct from the interaction of the heavier chalcogen elements (selenium, tellurium) and that sulfur represents a transition between these extrema.

The angle $\omega(y,\overline{X_1X_2})$ varies also within the families. The highest values within each family is always encountered for the system bearing oxygen on the accepting subunit (**1**, **5**, **9**, **13**, **17**, **21**, **25**, and **29**). The lowest values are found for **4**, **8**, **12**, **16**, **20**, **24**, **28**, and **32**, for which the accepting subunit carries tellurium. For those model systems containing oxygen in the donating subunit (**1**−**4** and **17**−**20**), the values for $\omega(y,\overline{X_1X_2})$ are always the lowest in each series if X_2 is held constant. It is also noted that, for those heteroatomic compounds having oxygen in the donating fragment, the angle $\omega(y,\overline{X_1X_2})$ deviates significantly from the ideal value of 90°, which one would expect for a p−σ*-type interaction (i.e., **4**: 62.3° and **20**: 43.6°).

The angle $\omega(z,\overline{X_2Z})$ decreases steadily in the families with Se or Te in the donor part, with the tellurium-containing acceptor fragment showing the smallest values. The average value for ω in these families varies between 22 and 36° for the CH_3 group, and between 18 and 28° for the CN group. Note that the strongest deviations from the ideal p−σ* model geometries occur for heteroatomic systems **5**, **9**, **13**, **21**, **25**, and **29**, where the accepting unit contains an oxygen atom.

The interaction energies $E_{int,MP2}^{cc-pVTZ-ECP}$ are higher for the model compounds bearing the electron-withdrawing substituent Z = CN (**17**−**32**) on the accepting subunit than they are for the acceptor bearing dimethyl ether or its sulfur, selenium, and tellurium congeners (**1**−**16**). It increases within each family when going from X_2 = O to X_2 = Te for the model compounds having a cyano substituent in the accepting fragment. The stabilization maximum for the heteronuclear pairs is calculated for **20** (−6.59 kcal/mol), **24** (−6.42 kcal/mol), and **28** (−6.44 kcal/mol). Common to all three pairs is a CH_3TeCN acceptor unit. These values are close to that found for the homonuclear pair **32** (−6.18 kcal/mol). $E_{int,MP2}^{cc-pVTZ-ECP}$ decreases slightly in the second group (**17**−**32**) when changing X_1 from O to X_1 = Te (X_2 = O, $\Delta E_{int,MP2}^{cc-pVTZ-ECP}$ = 0.2 kcal/mol; X_2 = S, $\Delta E_{int,MP2}^{cc-pVTZ-ECP}$ = 0.5 kcal/mol; X_2 = Se, $\Delta E_{int,MP2}^{cc-pVTZ-ECP}$ = 0.6 kcal/mol; X_2 = Te, $\Delta E_{int,MP2}^{cc-pVTZ-ECP}$ = 0.4 kcal/mol). However, the significance of this decrease should not be overemphasized, considering the sophistication of the theoretical level applied and the pitfalls encountered when investigating intermolecular interactions.

The families belonging to the first group (Z = CH_3) show a different behavior. Here, a slight increase in the interaction energy $E_{int,MP2}^{cc-pVTZ-ECP}$ is noted for X_2 = O (**1**, **5**, **9**, **13**), X_2 = S (**2**, **6**, **10**, **14**), X_2 = Se (**3**, **7**, **11**, **15**), and X_2 = Te (**4**, **8**, **12**, **16**).

The noncovalent interactions also modify the stretching vibration when compared with that of the monomers. As it was observed in our study on the homoatomic cases,[19] it was also found here that a significant change $\Delta\tilde{\nu}_{symm}$ is observed for the symmetric stretching mode of the X_2−C bond (Table 1). The most apparent trend observed for $\Delta\tilde{\nu}_{symm}$ is that, for the first group (**1**−**16**), the values are either positive (**1**: 4.6 cm^{-1} and **3**: 0.7 cm^{-1}) or scatter in the slightly negative

Table 2. Partition of Interaction Terms for Model Systems **1**−**32** as Derived by a NBO Second-Order Perturbation Analysis into Chalcogen−Chalcogen Interactions (E_{XX}) and Hydrogen Bonding (E_{H-bond})[a]

system	X_1	X_2	Z	E_{XX}[b]	E_{H-bond}[b]	CT	$E_{p-\sigma^*}$[b]
1	O	O	Me	0.1	2.2	−1.05	
2	O	S	Me	0.7	1.6	0.63	
3	O	Se	Me	2.8	1.1	2.23	0.5
4	O	Te	Me	4.5	1.0	4.65	1.2
5	S	O	Me	0.0	3.3	−1.54	
6	S	S	Me	0.5	2.7	0.06	
7	S	Se	Me	7.4	2.2	4.98	1.6
8	S	Te	Me	8.2	1.7	16.17	4.3
9	Se	O	Me	0.0	3.5	−0.77	
10	Se	S	Me	2.1	3.3	0.69	
11	Se	Se	Me	6.2	2.5	4.52	1.0
12	Se	Te	Me	8.5	2.3	15.16	3.3
13	Te	O	Me	0.4	2.5	2.15	
14	Te	S	Me	1.5	3.0	1.42	
15	Te	Se	Me	6.7	2.8	6.02	1.1
16	Te	Te	Me	5.9	2.3	14.91	3.8
17	O	O	CN	0.1	1.8	5.01	
18	O	S	CN	2.5	1.1	5.74	0.9
19	O	Se	CN	5.0	1.0	10.49	1.6
20	O	Te	CN	9.9	0.9	19.65	3.6
21	S	O	CN	0.0	2.7	7.64	
22	S	S	CN	3.4	1.3	12.49	1.8
23	S	Se	CN	7.0	1.1	24.11	4.2
24	S	Te	CN	16.8	1.2	52.09	11.8
25	Se	O	CN	0.1	3.1	8.83	
26	Se	S	CN	4.8	1.6	14.27	1.9
27	Se	Se	CN	8.0	1.5	26.28	4.0
28	Se	Te	CN	19.2	1.4	58.94	11.4
29	Te	O	CN	0.3	2.3	9.64	
30	Te	S	CN	3.9	1.8	16.33	2.0
31	Te	Se	CN	6.8	1.8	30.20	4.4
32	Te	Te	CN	17.5	1.5	67.22	12.3

[a] The strongest NBO interaction term for the model compounds dominated by chalcogen−chalcogen interactions is included ($E_{p-\sigma^*}$). All values are given in kcal/mol. The charge transfer (CT) from donating units ($(CH_3)_2X_1$) to accepting units ($(CH_3)_2X_2Z$) is given in units of 10^{-3} electrons. [b] Values in kcal/mol.

range ($|\Delta\tilde{\nu}_{symm}| \leq 3.4$ cm^{-1}). Considering the approximations done in the vibrational analysis, these differences should not be given much significance. However, the changes for the second group (**17**−**32**) are both larger ($|\Delta\tilde{\nu}_{symm}| \leq 29.0$ cm^{-1}) and do not show scatter. Instead, within each of the families **17**−**20**, **21**−**24**, **25**−**28**, and **29**−**32**, the last member (X_2 = Te) shows the largest decrease in $\Delta\tilde{\nu}_{symm}$. This is in line with our previous observations that these model systems also exhibit the largest interaction energies $E_{int,MP2}^{cc-pVTZ-ECP}$ within each family and, therefore, are expected to show the largest influence on the X_2−C stretching mode.

NBO Analysis. To discuss the bonding in **1**−**32**, we characterize the noncovalent interactions in these species in terms of hydrogen bonding and chalcogen−chalcogen interactions. To unravel the various contributions, we used NBO analyses. This was done for **1**−**32** by interpreting the sums of the second-order interaction terms of the Fock operator in the NBO basis in terms of hydrogen bonding or chalcogen−chalcogen interactions. These results are listed in Table 2. It should be noted that this approach is only performed on the HF−SCF level of theory and that only bonding interactions are considered. Nevertheless, we find the results of this approach useful for a qualitative discussion. It gives us an insight into the interaction of the important functional groups. In Figure 4, we show the relative contributions of hydrogen− and chalcogen−chalcogen bonding for **1**−**32** summed up to 100%.

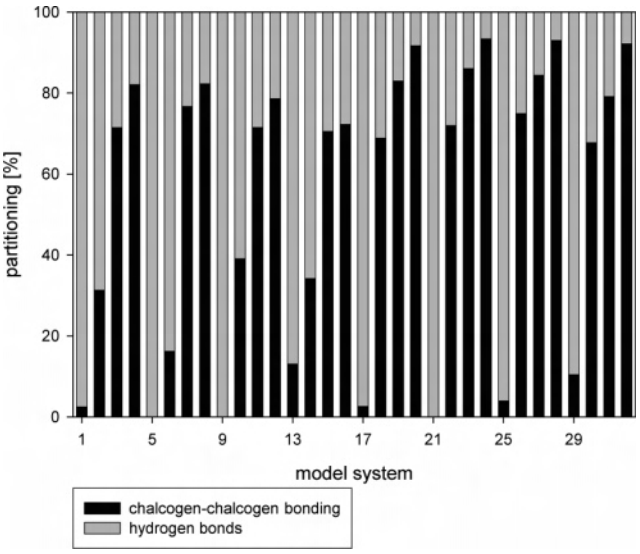

Figure 4. Relative contributions of the hydrogen− and chalcogen−chalcogen bonding, as derived from NBO calculations.

Figure 4 indicates that chalcogen−chalcogen interactions are increased when changing the substituent CH_3 in model compounds **1**−**16** to the electron-withdrawing group CN. It is seen that, for the first member of each family (oxygen-containing acceptor unit) in both groups, the hydrogen−chalcogen bonding prevails, to a vast extent, irrespective of the substituent on the accepting unit. For the first group (acceptor unit bears two methyl substituents), hydrogen bonding dominates also in those model systems in which the accepting unit is dimethyl sulfide (**2**, **6**, **10**, **14**), although to a lesser extent. For the corresponding model compounds in the second group (**18**, **22**, **26**, **30**), this is not the case. In these systems, the functional groups dominating the noncovalent bonding are the two chalcogen elements. This indicates, again, the transition-type behavior of sulfur, as was previously observed[19] and already described; the nature of the intermolecular interaction in the complexes having a sulfur-containing acceptor fragment changes, depending on the substituent of this unit. If the acceptor carries an electron-donating group, these model compounds behave similar to the oxygen congeners, while a (hard) electron-accepting group (Z = CN) results in behavior more like the heavier chalcogen elements Se or Te. These similarities between S−CN and Se−R or Te−R can be utilized in designing (supra)molecular architectures.[18]

It is interesting to note that, although the minimum conformation of two dimers may be similar (Table 1), the interaction in the dimers may differ significantly. This is pointed out in Figure 5, in which we have visualized the bonding linear combination of the corresponding p and σ^* orbitals of **29** and **30** at their minimum energy geometries. In **29**, the bonding between both units is due to three weak hydrogen bonds between the CH_3 group of the accepting dimethyl ether and the tellurium atom of the donating fragment. In contrast to this observation, the interaction

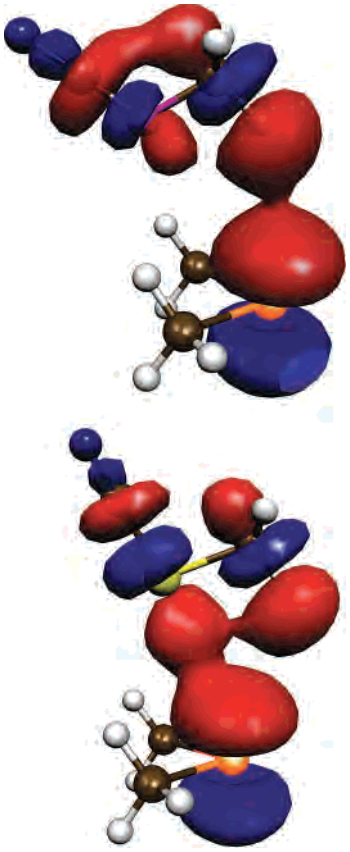

Figure 5. Minimum energy conformations of **29** (top) and **30** (bottom) along with the bonding linear combination of the relevant p and σ^* orbitals. The hydrogen bonds between the two methyl groups and the chalcogen atoms are not shown for the sake of clarity.

inherent in **30** is dominated by the van der Waals interactions between the sulfur and tellurium atoms. In **29**, there are two weak hydrogen bonds between the dimethyl tellurium and the oxygen (not shown for the sake of clarity) and one between one methyl group of CH_3OCN and the tellurium center. Similar hydrogen bonding is described in the literature.[43,44] The calculated geometry of **1**[19] is in good agreement with experiment.[44c] It is interesting to note (as shown in Figures 4 and 5) that there appears to be a continuum between p$-\sigma^*$ and hydrogen bonding interactions.

In Figure 6, the charge transfer (CT) in **1**−**32** from the donating units ($(CH_3)_2X_1$) to the accepting units (CH_3X_2-Z) is visualized. We observe a steady increase in each family, with the exception of the systems **13** and **14**. Model system **14** (1.42×10^{-3} electrons) shows a slightly smaller charge transfer than **13** (2.15×10^{-3} electrons). However, this difference, as well as the absolute values associated with the CT in these systems, is so small that this observation should not be overemphasized.

A huge difference is observed between the two groups **1**−**16** and **17**−**32**, that is, the influence of the substituent Z

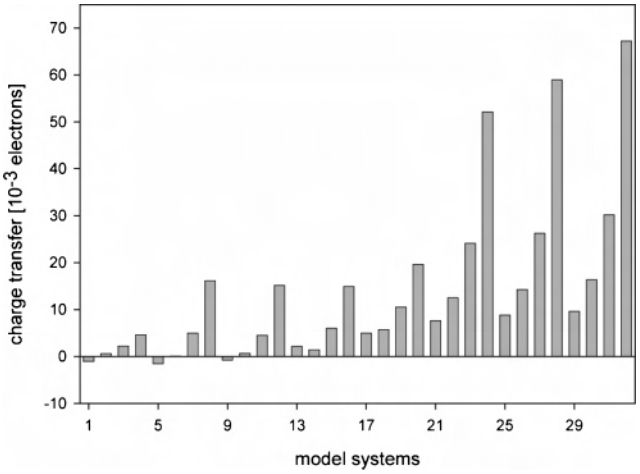

Figure 6. Charge transfer (CT) from the donating units ($(CH_3)_2X_1$) to the accepting units (CH_3X_2Z).

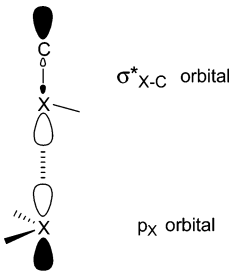

Figure 7. Directional bonding of two chalcogen centers in R−X−R′ by a p$-\sigma^*$ interaction.

on the extent of the bonding as mirrored in the CT data. The absolute values for the CT for the first group (Z = CH_3) range from 0.63 (**2**) to 16.17×10^{-3} electrons (**8**), while in the second group, values from 5.01 (**17**) to 67.22×10^{-3} electrons (**32**) are encountered.

It should be noted that these findings are not completely consistent with the interaction energies $E_{int,MP2}^{cc-pVTZ-ECP}$ discussed previously in this Article (Table 2). Although the general trends are reproduced (i.e., the increase of $E_{int,MP2}^{cc-pVTZ-ECP}$ when changing Z from CH_3 to CN), the charge as well as the net NBO interaction terms predict a significant increase in the interaction within the series **20**, **24**, **28**, **32**. However, the MP2/cc-pVTZ-ECP calculations deviate from this. This discrepancy should be due to the neglect of correlation effects in the NBO analyses as well as to the exclusion of any antibonding contributions.

Noncovalent interactions between divalent chalcogen moieties have, so far, been associated with a p$-\sigma^*$ molecular orbital interaction between the occupied np orbital of the donor chalcogen unit and the σ^* orbital of the X_2-Z bond of the acceptor. This interpretation stems from extended experimental investigations on chalcogen compounds[10] (Figure 7). In line with these views were HF−SCF[15] and DFT calculations.[25] However, our recent calculations on chalcogen−chalcogen interactions[19] and those of others[11,16] reveal that the inclusion of correlation effects is necessary to describe the bonding in systems such as **1**−**32** quantitatively. The well-established p$-\sigma^*$ molecular orbital model still proved sufficient to qualitatively explain the trends observed in our previous work. The inclusion of the mixed

(43) (a) Gu, Y.; Kar, T.; Scheiner, S. *J. Am. Chem. Soc.* **1999**, *121*, 9411−9422. (b) Alabugin, I. V.; Manoharan, M.; Peabody, S.; Weinhold, F. *J. Am. Chem. Soc.* **2003**, *125*, 5973−5987.

(44) (a) van der Veken, B. J.; Herrebout, W. A.; Szostak, R.; Shchepkin, D. N.; Havlas, Z.; Hobza, P. *J. Am. Chem. Soc.* **2001**, *123*, 12290−12293. (b) Delanoye, S. N.; Herrebout, W. A.; van der Veken, B. J. *J. Am. Chem. Soc.* **2002**, *124*, 7490−7498. (c) Tatamitani, Y.; Liu, B.; Shimada, J.; Ogata, T.; Ottaviani, P.; Maris, A.; Caminati, W.; Alonso, J. L. *J. Am. Chem. Soc.* **2002**, *124*, 2739−2743.

compounds (i.e., Te···Te, Te···Se, Se···Te, Se···Se) in this work allows a more profound examination of the reliability of this p−σ* model. The strongest NBO second-order interaction terms between the two molecular units are given in Table 2 (last column) for those compounds for which chalcogen−chalcogen interactions prevail. In all cases, these terms arise from p−σ*-type NBO interactions. Therefore, if one intentionally chooses the molecular orbital (MO) model to explain chalcogen−chalcogen interactions, one should use this established p−σ* model because this type of MO interaction provides the largest individual contribution to the interaction between two chalcogen atoms. Notwithstanding this fact, it should still be stressed that, due to the dominating dispersive character, the MO framework does not represent a fully justified description of chalcogen−chalcogen interactions.

It has already been observed[19] that the p−σ* model cannot give a quantitative explanation for the interaction energies observed for the homoatomic compounds. Despite this, qualitatively explaining the trends in a series of compounds was readily possible for the homoatomic model systems treated in that work. By inclusion of the heteroatomic compounds such as **2** to **4**, we find that even the explanation of trends in the interaction energies cannot be maintained. For example, the p−σ*-type orbital interaction $E_{p-\sigma^*}$ is ca. 3.5 times greater in **32** than it is in **20**, while the interaction energy $E_{int,MP2}^{cc-pVTZ-ECP}$ is larger for **20**.

Symmetry-Adapted Perturbation Theoretical (SAPT) Studies. Our recent studies on the interaction between pairs of homonuclear chalcogen compounds[19] and related studies by others[11,16] reveal that a highly correlated method is necessary to quantitatively describe the nature of so-called noncovalent bonding. Therefore, we adopted the terminology derived from the symmetry-adapted perturbation theoretical (SAPT)[38] treatment to partition the interaction into the four principal forces (electrostatic, induction, dispersion, and exchange).

In this approach, the interaction energy E_{int} is calculated as an (infinite) expansion consisting of four principal components termed electrostatic (E_{elst}), induction (E_{ind}), dispersion (E_{disp}), and exchange (E_{exch}) energies (eqs 2 and 3). For practical applications, each expansion coefficient $E_{SAPT}^{(n)}$ is approximated using a perturbation expansion from the HF wave function. In effect, this amounts to a double perturbation approach for the total interaction energy $E_{int,SAPT}$.

$$E_{int,SAPT} = \sum_{n=1}^{\infty} E_{SAPT}^{(n)} = \sum_{n=1}^{\infty}\sum_{k=0}^{\infty} E_{SAPT}^{(nk)} \qquad (2)$$

In practice, these infinite expansions are truncated after a finite number of terms, and in the presently available implementation (SAPT2002), $E_{int,SAPT}$ is calculated as

$$E_{int,SAPT} = E_{pol}^{(10)} + E_{exch}^{(10)} + E_{ind,resp}^{(20)} + E_{exch-ind,resp}^{(20)} + \delta_{HF} + \epsilon_{pol}^{(1)}(3) + \epsilon_{exch}^{(1)}(2) + E_{disp}^{(20)} + \epsilon_{disp}^{(2)}(2) + E_{exch-disp}^{(20)} \qquad (3)$$

To investigate the relative influence of the four principal forces, we have used eqs 4−7

$$E_{elst} = E_{pol}^{(10)} + E_{exch}^{(10)} + \epsilon_{pol}^{(1)}(3) \qquad (4)$$

$$E_{ind} = E_{ind,resp}^{(20)} + E_{exch-ind,resp}^{(20)} \qquad (5)$$

$$E_{disp} = E_{disp}^{(20)} + \epsilon_{disp}^{(2)}(2) + E_{exch-disp}^{(20)} \qquad (6)$$

$$E_{exch} = \epsilon_{exch}^{(1)}(2) \qquad (7)$$

to sum up several expansion coefficients, resulting in a partition of E_{int} into E_{elst}, E_{ind}, E_{disp}, and E_{exch}. For details on this partitioning, see ref 19 and the corresponding Supporting Information. The results of the SAPT calculations on **1**−**32** are summarized in Table 3 and are depicted in Figure 8. For all systems **1**−**32**, the SAPT2002/DGDZVP interaction energies $E_{int,SAPT}^{DGDZVP}$ correlate well with those obtained at the MP2/cc-pVTZ-ECP level of theory (see the Supporting Information for details).

The electrostatic force contributes in a bonding manner in all complexes having at least one oxygen-containing fragment (**1**−**5**, **9**, **13**, **17**−**21**, **25**, **29**). However, with the exception of the systems **17**−**20**, the actual contribution remains rather constant compared to that of the other forces, ranging from −0.30 (**3**) to −0.68 kcal/mol (**21**). Only in **17**−**20** does the contribution exceed this range significantly, and an increase is observed when going from **17** (X_2 = O, −1.22 kcal/mol) to **20** (X_2 = Te, −2.09 kcal/mol).

All systems not containing oxygen atoms show a different behavior. Here, the bonding contribution of the electrostatic interaction decreases with an increased atomic number of X_2, while a dependence on the chalcogen element X_1 as well as the substituent Z is observed. The remaining systems in the first group (Z = CH_3), show a bonding electrostatic interaction whenever the acceptor fragment contains sulfur, with a decrease in bonding when going from X_1 = S to X_1 = Te. Antibonding contributions are found for X_2 = Se, Te; also here, an increase in antibonding character is found when changing X_1 from S to X_1 = Te. Substituting Z = CH_3 for Z = CN leads to an increased amount of electrostatic interaction, while the bonding character is not changed. The only exception to this is system **23**, which shows a bonding electrostatic contribution (−0.26 kcal/mol), while the corresponding first group system **7** exhibits a slight antibonding electrostatic character (+0.04 kcal/mol). Overall, we observe a different behavior in those model compounds containing an oxygen atom in the donating fragment (**1**−**4**, **17**−**20**), which show bonding electrostatic interactions irrespective of the acceptor's chalcogen element. For all other families, a bonding contribution of the electrostatic interaction is observed for the first member (X_2 = O), and a strong antibonding contribution is observed for the last (X_2 = Te). The systems with S or Se in the acceptor fragment exhibit intermediate behavior.

The induction force is bonding in each model system, and a huge difference between the two groups is observed. In the first group (Z = CH_3), bonding due to induction is rather small and constant within each family, ranging only from −0.24 (**6**) to −0.55 kcal/mol (**4**). This is contrary to the contribution in the second group (Z = CN), in which a clear-

Table 3. Contribution of the Electrostatic (E_{elst}), Induction (E_{ind}), Dispersion (E_{disp}), and Exchange Correlation (E_{exch}) Energies to the Interaction Energy $E_{int,SAPT}^{DGDZVP}$ on MP2/DGDZVP-Optimized Geometries, as Derived by the SAPT2002 Program and Summed According to eqs 4−7[a]

system	X_1	X_2	Z	E_{elst}	E_{ind}	E_{disp}	E_{exch}	$E_{int,SAPT}^{DGDZVP}$ [b]
1	O	O	Me	−0.42	−0.35	−1.80	0.72	−2.04
2	O	S	Me	−0.39	−0.31	−1.79	0.64	−2.03
3	O	Se	Me	−0.30	−0.37	−2.23	0.93	−2.21
4	O	Te	Me	−0.39	−0.55	−2.68	1.43	−2.56
5	S	O	Me	−0.50	−0.40	−1.91	0.69	−2.37
6	S	S	Me	−0.18	−0.24	−1.68	0.33	−1.97
7	S	Se	Me	0.04	−0.25	−1.99	0.43	−1.99
8	S	Te	Me	0.30	−0.40	−2.40	0.73	−2.11
9	Se	O	Me	−0.52	−0.43	−2.08	0.77	−2.53
10	Se	S	Me	−0.12	−0.26	−1.86	0.38	−2.08
11	Se	Se	Me	0.18	−0.27	−2.22	0.50	−2.08
12	Se	Te	Me	0.60	−0.48	−2.76	0.87	−2.17
13	Te	O	Me	−0.55	−0.44	−2.17	0.83	−2.62
14	Te	S	Me	−0.05	−0.26	−1.97	0.42	−2.11
15	Te	Se	Me	0.29	−0.28	−2.35	0.53	−2.11
16	Te	Te	Me	0.74	−0.49	−2.87	0.89	−2.15
17	O	O	CN	−1.22	−0.39	−1.77	0.79	−2.83
18	O	S	CN	−1.62	−0.64	−2.27	1.24	−3.67
19	O	Se	CN	−1.91	−0.94	−2.79	1.78	−4.39
20	O	Te	CN	−2.09	−1.56	−3.45	2.64	−5.30
21	S	O	CN	−0.68	−0.26	−1.70	0.44	−2.43
22	S	S	CN	−0.49	−0.40	−1.95	0.52	−2.68
23	S	Se	CN	−0.26	−0.70	−2.44	0.85	−3.10
24	S	Te	CN	0.40	−1.71	−3.22	1.58	−3.88
25	Se	O	CN	−0.60	−0.28	−1.86	0.50	−2.50
26	Se	S	CN	−0.26	−0.42	−2.18	0.58	−2.68
27	Se	Se	CN	0.19	−0.80	−2.82	1.00	−3.09
28	Se	Te	CN	1.26	−2.24	−3.85	1.92	−3.96
29	Te	O	CN	−0.49	−0.25	−1.93	0.52	−2.41
30	Te	S	CN	−0.07	−0.41	−2.22	0.57	−2.53
31	Te	Se	CN	0.42	−0.78	−2.84	0.96	−2.89
32	Te	Te	CN	1.68	−2.34	−3.93	1.86	−3.72

[a] All values are given in kcal/mol. [b] This column collects the sum of the four contributions plus δ_{HF}. For details, see Supporting Information.

cut dependence on the accepting chalcogen element X_2 is observed. Here, the bonding contribution increases within each family, ranging from −0.39 to −1.56 (**17**−**20**), −0.26 to −1.71 (**21**−**24**), −0.28 to −2.24 (**25**−**28**), and −0.25 to −2.34 kcal/mol (**29**−**32**). However, comparing the two groups, we note that the contribution of induction to the bonding is not highly influenced by the substituent Z whenever the acceptor unit contains either oxygen or sulfur atoms. This reflects the higher polarizability of Se and Te in comparison with that of O or S.

The dispersion force contributes most to the bonding in all systems **1**−**32**, and it contributes most for the last member in each family. Similar to induction, its contribution remains rather constant for those compounds in which the accepting fragment contains either oxygen (**1**, **5**, **9**, **13**, **17**, **21**, **25**, **29**) or sulfur atoms (**2**, **6**, **10**, **14**, **18**, **22**, **26**, **30**). In these compounds, it ranges only from −1.70 (**21**) to −2.17 (**13**) and from −1.68 (**6**) to −2.27 kcal/mol (**18**). These findings reflect the poor polarizabilities of these two elements. For the compounds containing either Se or Te in the accepting unit, the contribution is increased upon changing Z from CH_3 to CN, reflecting the higher polarizabilities of Se and Te with respect to those of O and S. However, within each group, the contributions also remain rather constant when keeping X_2 constant.

Exchange contributions are repulsive for all model systems **1**−**32**. For the first group, the repulsive contribution is minimal in each family for the systems containing sulfur as the accepting chalcogen (**2**, **6**, **10**, **14**). In the second group, it increases in each family with the atomic number of the accepting chalcogen.

Noncovalent bonding between oxygen and selenium is a well-established example of chalcogen−chalcogen interactions[21c,22a] and was attributed to a dominating electrostatic force by analysis of ab initio and/or NMR investigations.[26] Similar investigations were performed on a variety of noncovalent interactions involving at least one chalcogen atom.[45] As it is apparent from Table 3 and Figure 8, the electrostatic forces prevalent in systems **3** and **19** indeed indicate electrostatic contributions to the chalcogen−chalcogen bonding in these compounds. However, we note that, in both systems, the dominating force actually is of dispersive and not of electrostatic character and that the electrostatic contribution is largely controlled by the electron-withdrawing capabilities of the substituent Z adjacent to the Se−C bond in the acceptor fragment.

It is highly enlightening to compare these two model systems, **3** and **19**, with their oxygen and selenium homologues (**1**, **17** and **11**, **27**). As is indicated by NBO analyses, there is a predominance of weak hydrogen bonds in the oxygen compounds **1** and **17** (∼97% hydrogen bonding in both), while chalcogen−chalcogen interactions prevail in the mixed compounds (72 (**3**) and 83% (**19**) chalcogen bonding) as well as in the selenium-containing ones **11** (72% chalcogen bonding) and **27** (85% chalcogen bonding). This indicates that the nature of the intermolecular bond in **1** and **17** should be similar to each other but different from **3**, **11**, **19**, and **27**. At the same time, the equivalent compounds from the two groups (**3**, **19** and **11**, **27**) should show similar properties in their intermolecular interaction, as indicated by the highly similar magnitude of the chalcogen-type interaction. We note from Table 2 and Figure 8 that this is, indeed, the case. The only significant difference in the nature of the intermolecular bond of these six particular model systems is actually in the bonding or repulsive contribution of the electrostatic force. As previously stated,[19] electrostatic interactions contribute in a bonding manner in all oxygen-containing systems **1**, **3**, **17**, and **19**, while in the selenium congeners **11** and **27**, its influence is repulsive. This finding indicates that a bonding electrostatic force is not indicative of weak hydrogen bonds, as one might have been compelled to conjecture if confined to the homoatomic model compounds only. In these homoatomic compounds, electrostatic forces only contribute in a bonding manner when hydrogen bonding prevails. Thus, it is clearly shown that prevalent chalcogen−chalcogen interactions can also establish a significant bonding of electrostatic nature and, thus, are not limited solely to dispersive- or inductive-type forces.

(45) (a) Iwaoka, M.; Tomoda, S. *J. Am. Chem. Soc.* **1996**, *118*, 8077−8084. (b) Iwaoka, M.; Komatsu, H.; Katsuda, T.; Tomoda, S. *J. Am. Chem. Soc.* **2002**, *124*, 1902−1909. (c) Iwaoka, M.; Katsuda, T.; Tomoda, S.; Harada, J.; Ogawa, K. *Chem. Lett.* **2002**, *5*, 518−519. (d) Nakanishi, W.; Hayashi, S.; Sakaue, A.; Ono, G.; Kawada, Y. *J. Am. Chem. Soc.* **1998**, *120*, 3635−3640.

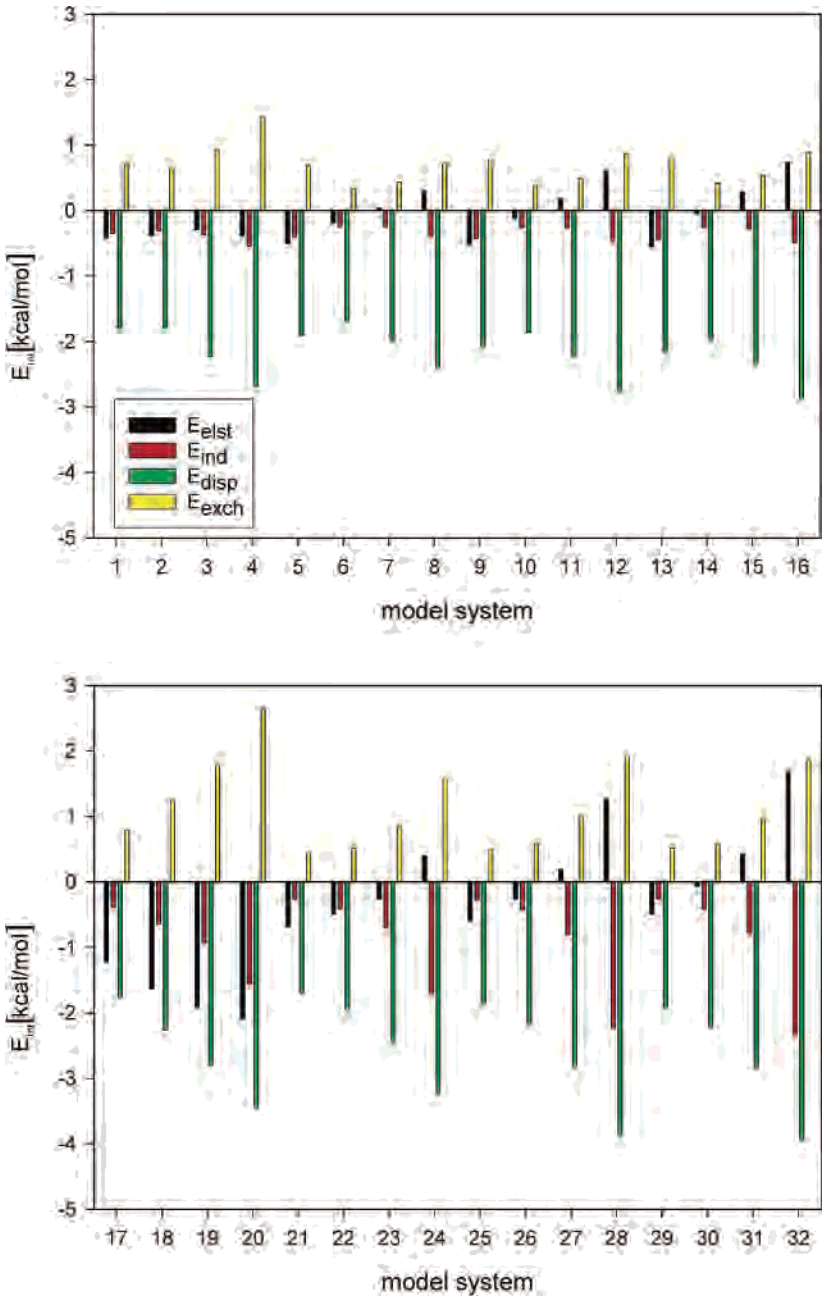

Figure 8. Contribution of the electrostatic (E_{elst}), induction (E_{ind}), dispersion (E_{disp}), and exchange correlation (E_{exch}) energies to the interaction energy $E_{int,SAPT}^{DGDZVP}$, as derived by the SAPT2002 program and summed according to eqs 4−7.

It is also seen that the very prerequisite for bonding electrostatic contribution to chalcogen−chalcogen interactions is the involvement of hard chalcogen centers. This fact is very elaborately seen in the tellurium analogues **4**, **16** and **20**, **32** in contrast to the selenium- and/or oxygen-containing compounds **3**, **11** and **19**, **27**. For both **16** and **32**, we note a dominating chalcogen−chalcogen interaction accompanied by both a strongly bonding dispersion as well as a strongly repulsive electrostatic-type force. It is illustrative to note that the electrostatic force in **16** is less repulsive than that in **32**, the latter having the stronger electron-withdrawing substituent in the acceptor fragment. This is in contrast to the mixed oxygen−tellurium systems **4** and **20**, in which chalcogen−chalcogen interactions prevail as well but which also show bonding significant electrostatic contributions to the intermolecular bonding. More interestingly, the stronger electron-withdrawing substituent in **20** increases the bonding due to electrostatic forces when compared to **4** as mentioned previously in this Article. This stands in clear contrast to the pair **16** and **32**.

Therefore, it is clearly shown that the nature of chalcogen−chalcogen interactions is not limited to a dispersive-type character and that electrostatic contributions are not necessarily repulsive in nature. However, for a significant electrostatic nature of the noncovalent bonding, at least one of the chalcogens must be hard, such as in **3**, **4**, **19**, and **20**. However, the donor does not necessarily have to be hard, as can be seen from the pairs **3**, **9** and **4**, **13**. When having a hard chalcogen, an electron-withdrawing substituent increases the bonding due to electrostatic interactions. On the other

hand, hydrogen-bonded systems are indicative of a (strongly) bonding electrostatic contribution. In each of the model systems with prevailing hydrogen bonding (**1**, **2**, **5**, **6**, **9**, **10**, **13**, **14**, **17**, **21**, **25**, **29**), the electrostatic force is significantly bonding. However, it should be stressed at this point that the major bonding contribution stems from the dispersion interaction in all systems **1**−**32**. For this reason, the intermolecular bond in these systems should not be considered as electrostatic in origin, although electrostatic interactions indeed may play a bonding role.

Concluding Remarks

This study extends our previous investigation on noncovalent interactions between two fragments containing divalent chalcogen atoms to heteroatomic model systems. The same techniques were applied as previously, including supermolecular interaction energies (MP2/cc-pVTZ-ECP), NBO (HF/aug-cc-pVTZ-ECP), as well as perturbation theoretical (SAPT2002/DGDZVP) analyses.

The findings are in keeping with our previous results. They show an increase in the interaction energy in each of the families **1**−**4**, **5**−**8**, **9**−**12**, **13**−**16** and **17**−**20**, **21**−**24**, **25**−**28**, **29**−**32** when changing X_2 from O via S and Se to Te. An increase in the interaction energy is also observed when changing the substituent Z on the acceptor fragment from CH_3 to CN. The most strongly bound systems are, in each family, the tellurium-containing systems ($E_{\mathrm{int,MP2}}^{\mathrm{cc-pVTZ-ECP}} \approx 3$ (first group) and 6 kcal/mol (second group)), while the oxygen (or sulfur)-containing analogues exhibit the lowest interaction ($E_{\mathrm{int,MP2}}^{\mathrm{cc-pVTZ-ECP}} \approx 2-3$ kcal/mol). Hydrogen bonds prevail only in those compounds which contain oxygen or sulfur atoms in the accepting fragment (**1**, **2**, **5**, **6**, **9**, **10**, **13**, **14**, **17**, **21**, **25**, **29**) but never when selenium or tellurium atoms are in the accepting subunit. This holds true even if the accompanying chalcogen atom is an oxygen (i.e., **3**, **4**, **18**−**20**). The importance of chalcogen−chalcogen interactions increases in each family with increased atomic weight of the accepting chalcogen atom, that is, in the series X_2 = O → S → Se → Te. Perturbation theoretical analyses (SAPT2002/DGDZVP) reveal a dominating dispersion interaction in all systems **1**−**32**, in line with our previous results. All hydrogen-bonded systems exhibit bonding electrostatic contributions, with the electron-withdrawing substituted systems of the second group (**17**, **21**, **25**, **29**) showing a greatly increased electrostatic character when compared to that of the members of the first group (**1**, **2**, **5**, **6**, **9**, **10**, **13**, **14**). Dominating chalcogen−chalcogen interactions can involve both bonding as well as antibonding electrostatic characters. However, bonding electrostatic character in chalcogen−chalcogen interaction-dominated compounds is observed only if at least one of the chalcogen atoms is oxygen or sulfur (**3**, **4**, **18**−**20**, **22**, **23**, **26**, **30**).

It was already noted in our previous study[19] that the p−σ* model does not give a quantitative explanation of the interaction energy between two chalcogen moieties. Especially considering the data of the heteroatomic model systems of this work, the p−σ* model should be taken with some amount of skepticism. Nevertheless, even such an imperfect model has been appropriate enough to reproduce, with good accuracy, trends and details of structures that exhibit this type of interaction.

Acknowledgment. In memoriam of Professor Edgar Heilbronner. This research was supported by the Deutsche Forschungsgemeinschaft (DFG) and the Fonds der Chemischen Industrie. D.B.W. is grateful to the Graduiertenkolleg 850 (Molecular Modeling) and to the Studienstiftung des deutschen Volkes for a graduate fellowship. C.B. is grateful to the International Ph.D. program of the German Cancer Research Center for a graduate fellowship.

Supporting Information Available: Cartesian coordinates, absolute energies for all compounds **1**−**32**, details of the SAPT calculations, a detailed description of SAPT and NBO summation algorithms. This material is available free of charge via the Internet at http://pubs.acs.org.

IC062110Y